

THE STRUCTURE OF H₂O MASERS ASSOCIATED WITH LATE-TYPE STARS

J. H. SPENCER AND K. J. JOHNSTON

E. O. Hulburt Center for Space Research, Naval Research Laboratory

J. M. MORAN AND M. J. REID

Harvard-Smithsonian Center for Astrophysics

AND

R. C. WALKER

Massachusetts Institute of Technology

Received 1978 November 6; accepted 1978 December 15

ABSTRACT

The H₂O maser emission features for each of the stars RT Vir, W Hya, RX Boo, and RR Aql have been found to lie in a region $\leq 1 \times 10^{14}$ cm. The masers are probably located in a shell surrounding the star. There have been order-of-magnitude variations in the flux densities of these H₂O masers since 1973, and we expect there should have been variations in the infrared flux of these stars if the masers are pumped by IR photons. Weak, broad, quasi-thermal features are found to underlie the narrow features in W Hya, RX Boo, and R Aql.

Subject headings: masers — stars: circumstellar shells — stars: late-type — stars: long-period variables

I. INTRODUCTION

H₂O maser emission associated with long-period variable stars has been studied by Schwartz, Harvey, and Barrett (1974); Dickinson (1976); Rosen *et al.* (1978); Lepine, Paes de Barros, and Gammon (1976), among others. Stars that display H₂O emission also have associated OH masers. These include the Mira long-period variables, giant semi-regular variables, and M supergiants. The only star whose maser H₂O emission has been studied with high angular resolution is VY CMa (Rosen *et al.* 1978). In order to learn more about the energy mechanisms of the masers and mass loss of these late-type stars, high-resolution observations were made of the H₂O masers associated with these objects.

II. OBSERVATIONS AND RESULTS

The 26 m telescope at the Maryland Point Observatory of the Naval Research Laboratory was used between 1976 September 7 and 10 to observe the 34 infrared stars with known H₂O maser emission which are listed in Table 1. The purpose of these observations was to select the five most intense H₂O sources associated with M stars. At this time the receiver was an RF maser amplifier giving a system temperature of approximately 200 K. All observations were taken in a beam-switched mode with a spectrometer consisting of 96 adjacent 50 kHz (0.67 km s⁻¹) filters. The observations of Table 1 are the first confirming observations for many of these sources.

Based on these measurements, a VLBI experiment was conducted on RT Vir, W Hya, RX Boo, R Aql, and RR Aql between 1976 September 16 and 20. The

interferometer elements were the 26 m telescope at Maryland Point, Maryland, the 43 m telescope of the NRAO,¹ located in Green Bank, West Virginia, and the 37 m Haystack Observatory antenna in Westford, Massachusetts. Difficulties with the maser amplifier at Maryland Point at the time of the VLBI experiment forced the use of a mixer radiometer with a system temperature of 2000 K. The radiometers at Haystack and NRAO consisted of maser and parametric amplifiers with typical system temperatures of 180 K and 630 K, respectively. All local oscillators were locked to hydrogen maser frequency standards. The standard Mark II tape recorder system was used (Clark 1973), and the video tapes were processed at the NRAO in Charlottesville, Virginia.

The initial output of the processor was a cross-correlated spectrum of 128 channels (96 independent) over a 2 MHz bandwidth, with a velocity resolution of 0.34 km s⁻¹ (uniform weighting). The data were coherently averaged over a 1–30 s period, depending on the desired field of view. For all the stars, we initially used large fields of view ($\sim 10''$) and narrowed the windows only after locating fringes. A strong spectral feature was selected as a reference, and its phase was subtracted from the other features. It was then possible to Fourier transform the data in each 30 minute scan to obtain relative fringe rate data and to produce fringe rate maps of the position of each spectral feature relative to the position of the reference feature (Moran 1973).

¹ The National Radio Astronomy Observatory is operated by Associated Universities, Inc., under contract with the National Science Foundation.

TABLE 1
STARS OBSERVED AT THE NRL MARYLAND
POINT OBSERVATORY

Name	IRC No.	Flux (Jy)
Y Cas.....	60 001	< 9*
CIT 3.....	10 011	14
o Cet.....	00 030	< 9
S Per.....	60 088	32
NML Tau.....	10 050	10
W Eri.....	-30 033	11
R Tau.....	10 060	< 12
	50 137	< 8
U Ori.....	20 127	< 12
VY CMa.....	-30 087	250
Z Pup.....	-20 133	< 10
R LMi.....	30 215	< 8
R Leo.....	10 215	39
V Ant.....	...	< 10
R Crt.....	-20 222	13
	-30 182	< 16
U CVn.....	40 238	< 8
RT Vir.....	10 262	107
W Hya.....	-30 207	104
RU Hya.....	-30 215	< 9
RX Boo.....	30 257	91
S CrB.....	30 272	29
U Her.....	20 298	32
VX Sgr.....	-20 431	31
R Aql.....	10 406	96
RR Aql.....	00 458	282
SY Aql.....	10 450	10
NML Cyg.....	40 448	26
UX Cyg.....	30 464	16
TW Peg.....	30 481	< 10
SV Peg.....	40 501	< 9
R Peg.....	10 527	8
PZ Cas.....	60 417	13
R Cas.....	50 484	< 6

* Limit is the peak-to-peak value of the spectrum.

To obtain the absolute maser positions, no phase referencing was done and only short integrations were used. A 40 level model atmosphere (based on the Air Research Defense Command Standard Atmosphere) was used to model the fringe rate residuals due to the atmosphere which were removed from the data, and the fringe rates were analyzed by the method of least squares to find the best estimate of right ascension and declination for the reference feature of each star.

Because there are not enough data to simultaneously solve for baseline, we adopted the baselines of Mader and Johnston (1973) (BX = -609529.7 m, BY = 467210.2 m, BZ = -352759.0 m). The resultant stellar positions are listed in Table 2. The measurements show no significant offsets between the masers and the associated stars.

After each scan, 5 minutes of bandpass data were taken so that the single antenna spectra could be properly calibrated and used to calibrate the normalized fringe visibilities. A representative autocorrelation spectrum for each star is given in Figure 1.

No fringes were detected from R Aql. The features in all the spectra of Figure 1 have low visibilities suggesting large sources or blends of many smaller sources. While in some sources there are features well separated in velocity (i.e., RT Vir), only in W Hya was it possible to detect cross-correlated flux from secondary features. Thus the fringe rate maps gave the relative position of the emission in each frequency channel across the main blended feature for all but W Hya. The individual masers that constitute a blend were all found to be within 0.05 of the reference channel. In the case of W Hya, the two features were separated by less than 0.04.

The size of the individual masers is determined by examination of the fringe visibility, the ratio of the correlated flux density to the total flux density. We find the sizes given in Table 3 for the strongest channel based on an assumption of a circular Gaussian shape. The limited sample of data does not merit or support more complicated analysis of spot structure.

III. DISCUSSION

The size and distribution of H₂O masers associated with late-type stars differ greatly from that reported for H₂O masers in H II regions (Johnston *et al.* 1977; Moran *et al.* 1973; Genzel *et al.* 1978) and even the H₂O masers in the direction of VY CMa (Rosen *et al.* 1978). The stellar masers have larger apparent angular sizes and lower total luminosities and brightness temperatures, and they are distributed over a much smaller region than the other objects. This is not unexpected because the masers in H II regions are sites of recent star formation, containing large amounts

TABLE 2
POSITIONS OF OBSERVED STARS*

SOURCE	RADIAL VELOCITY (km s ⁻¹)	RADIO POSITION (1950)		OPTICAL POSITION (1950)	
		α	δ	α	δ
RT Vir.....	22.5	13 ^h 00 ^m 05 ^s .65 ± 0.07	5°27'22".1 ± 6".2	13 ^h 00 ^m 05 ^s .70	5°27'15".2
W Hya.....	38.6	13 46 12.07 ± 0.14	-28 07 8.5 ± 1.3	13 46 12.22	-28 07 6.5
RX Boo.....	5.9	14 21 56.51 ± 0.05	25 55 50.0 ± 1.5	14 21 56.69	25 55 48.5
R Aql.....	19 03 57.67	-8 09 10.3
RR Aql.....	25.9	19 55 00.21 ± 0.07	-2 01 34.0 ± 14.2	19 55 00.2 ± 0.1†	-2 01 19.3 ± 1.0*

* Optical positions are taken from the SAO star catalog. The radio positions have been corrected for the listed proper motion for the date of observations.

† Based on measurement from National Geographic Society—Palomar Observatory Sky Survey.

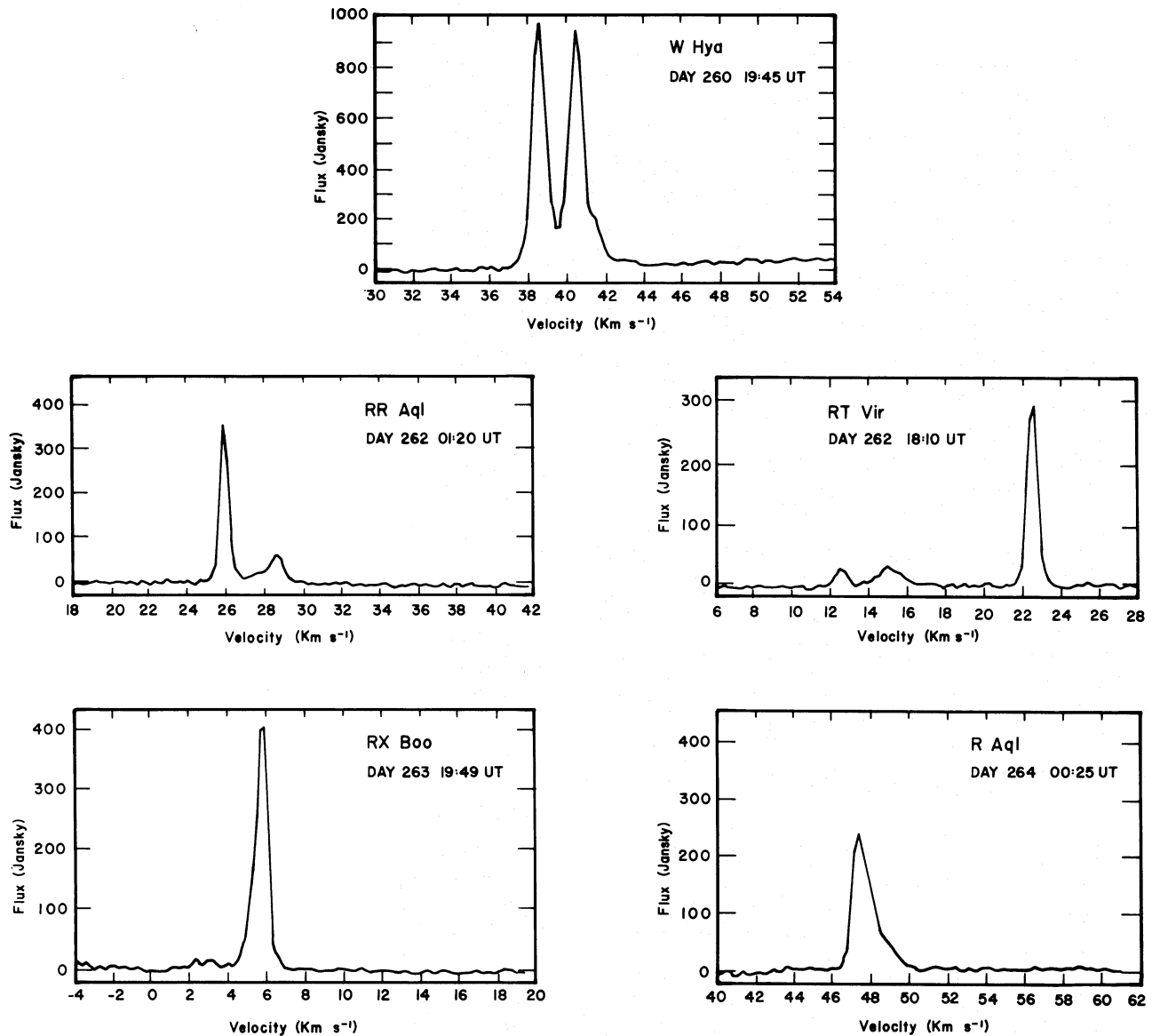


FIG. 1.—Spectra of the five stars observed in 1976 September. The rest frequency of the H₂O transition is 22235.08 MHz. The velocity resolution is 0.34 km s⁻¹.

TABLE 3
CHARACTERISTICS OF STARS OBSERVED

STAR	<i>mp</i>	<i>I</i> − <i>K</i>	DISTANCE (pc)	RADIAL VELOCITY OF FEATURE (km s ⁻¹)	<i>S</i> (Jy)	VISIBILITY (Hay- NRAO)	SIZE OF MASER FOR GAUSSIAN DISK		<i>T_B</i> (× 10 ¹¹ K)	MICROWAVE POWER OF FEATURE (× 10 ²² ergs s ⁻¹)
							(milli- arcsec)	(cm × 10 ¹³)		
RT Vir....	9.0–10.3	4.4	463	22.5	303	0.5	1.6	1.1	4.2	4.6
W Hya....	7.7–11.6	...	154	38.6	981	0.2	2.3	0.5	6.6	1.7
				40.5	954	0.2	2.3	0.5	6.4	1.6
RX Boo...	8.6–11.3	4.6	460	5.9	407	0.1	2.7	1.8	2.0	6.2
R Aql.....	5.7–12.0	5.0	295	47.4	237	1.5
RR Aql...	7.8–14.5	4.6	527	25.9	353	0.2	2.3	1.8	3.9	7.0

of dust and gas, and are thought to contain one or more massive O stars. The masers in late-type stars are probably located in a spherically symmetric expanding envelope surrounding the star, the result of mass loss from the star. The masers are located close to the star where the energy density is high enough to pump them, and the brightness temperature is less than H II region masers because the available energy and the density of H₂O is not high enough to create high-gain paths which would lead to smaller observed spot sizes for the masers.

Three of the stars studied are Mira variables, while the other two are semi-regular M type giants. Comparison of the spatial distribution of maser radiation of these stars with the supergiant VY CMa is also dramatic. The H₂O radiation associated with this supergiant is spread over an area of diameter 0".2 (5×10^{15} cm, assuming VY CMa is at a distance of 1500 pc), with individual masers having sizes of 1.5×10^{13} cm. While sizes of the individual masers are comparable, the size of the overall masing region is two orders of magnitude smaller for the masing regions reported in this paper.

The average brightness temperature for the masers studied is 4×10^{11} K. If the masers lie in regions 10^{14} cm radius from the star, i.e., $T \sim 10^3$ K, there are 20 gain lengths for an unsaturated maser. For a spherical unsaturated maser, the apparent size is related to the true size by

$$D_{\text{apparent}} = D_{\text{true}} \left(\frac{\log 2}{\alpha D_{\text{true}}} \right)^{1/2}$$

(Lang and Bender 1973). Since $\alpha D_{\text{true}} = 20$, the observed source size will be 5 times smaller than the true size. For 1000 K and this exponential gain, we expect the line width to be 0.4 km s^{-1} . The observed lines (see Fig. 1) are all $\geq 0.7 \text{ km s}^{-1}$. Therefore the temperature in the line-forming region must be doubled or the gain decreased to five in order to produce the observed line widths, although velocity structure in the masing region can also contribute to the observed line widths.

The assumption of unsaturated masers may be a good one because the strongest lines appear to be very slightly saturated. A maser is saturated when the stimulated emission rate exceeds the transition rates connecting the maser transition levels to other rotational levels in the molecule. These transition rates are about 1 s^{-1} (de Jong 1973) for the water molecule. An estimate of the stimulated emission rate at the surface of a maser can be obtained from

$$BJ_s = BJ_E D^2 / R^2$$

(Walker *et al.* 1978), where J_E = flux density at the Earth, D is the distance from the earth to the maser, R is the radius of the maser, and $B = 1.2 \times 10^7 \text{ cm}^2 \text{ ergs}^{-1} \text{ s}^{-1}$, the Einstein coefficient, and J_s is the radiation intensity averaged over all directions at the surface of the maser. For the maser in W Hya, $J_E = 1000 \text{ Jy}$, $D = 154 \text{ pc}$, $R = 3 \times 10^{13} \text{ cm}$, and the

surface stimulated emission rate is 34 s^{-1} . For the other sources, the surface-stimulated emission for the strongest lines may be 5 times that of W Hya. Thus, the strongest lines in the stellar maser spectra are saturated. This discussion holds for most nearly spherical geometries. For the masers associated with the H II region W51, the surface-stimulated emission was $5 \times 10^3 \text{ s}^{-1}$ (Walker *et al.* 1978); thus the saturation in these stars is not as intense as that of the masers associated with H II regions. The weaker maser lines may not be saturated. The saturation is small enough that the estimate for the size of the masers of $\sim 3 \times 10^{13} \text{ cm}$ obtained for an unsaturated maser is probably close to the correct size for the stellar H₂O masers, because most of the gain occurs in the unsaturated core rather than on the saturated surface.

The physical size of the masing regions having a size of $\sim 10^{14} \text{ cm}$ agrees well with models for H₂O emission, but forces some modifications. Olmon (1977) has classified long-period Mira variable stars which display maser emission according to their $I - K$ index. For stars with $(I - K) < 6$, i.e., RT Vir, RX Boo, and RR Aql, the maser emission should be confined to a narrow velocity interval, $\Delta v \leq 6 \text{ km s}^{-1}$, in a thin shell close to the star with a high kinetic temperature. This was true for the early observations available to Olmon, but our new observations with greater sensitivity show emission over 10 km s^{-1} for RT Vir and RX Boo. The masing region is probably on the innermost part of the dust envelope surrounding the star or may even be inside it. These stars have diameters similar to α Ceti and R Leo which were recently measured to be $\sim 10^{13} \text{ cm}$ (Labeyrie *et al.* 1977), thus the masers are probably 10 radii from the star's center. Assuming a mass-loss rate of $3 \times 10^{-6} M_\odot \text{ yr}^{-1}$, a ratio of 1000 for atomic hydrogen to water vapor (Goldreich and Scoville 1976), a shell masing region of radius 10^{14} cm with gas moving through it away from the star at 5 km s^{-1} (Dickinson *et al.* 1978), we obtain a number density of H₂O molecules in the shell of 10^6 cm^{-3} . This is three orders of magnitude less than the masers in massive H II regions (Walker *et al.* 1978).

The emission from the $J = 2-1$ transition of the ground vibrational state of SiO defines the stellar radial velocity (Dickinson *et al.* 1978). For the case of W Hya, the stellar velocity is $40.0 \pm 0.5 \text{ km s}^{-1}$ and the expansion velocity is $8.6 \pm 0.7 \text{ km s}^{-1}$. The narrow features we observe are at 38.6 and 40.5 km s^{-1} . Thus, this maser emission is coming from velocity regions close to the star. If it were coming from the front and back of the circumstellar shell, some of the backside emission would be blocked by the star if the stellar radius were as large as generally assumed ($4 \times 10^{13} \text{ cm}$ [Allen 1973]), but the spectra of RT Vir and RX Boo show strong redshifted (backside) components. Thus this observation is consistent with the recent results that the radii of Mira variables are $5 \pm 8 \times 10^{12} \text{ cm}$ (Labeyrie *et al.* 1977).

Schwartz *et al.* (1974) studied five long-period variables before 1973 May and found a correlation between the visual, infrared, and H₂O maser flux. The

TABLE 4
COMPARISON OF FLUX DENSITIES FOR
LONG-PERIOD VARIABLES

Star	Max-Min (Schwartz <i>et al.</i> 1974) (Jy)	This Paper (Jy)
R Aql.....	800-100	138-237
U Her.....	500-100	32
W Hya.....	350-100	1000-2000
S Cr B.....	100-50	29
U Ori.....	1600-500	< 12

H₂O emission was found to be periodic with the same period as that of the stellar luminosity variation with no phase lag between the H₂O maser and infrared flux. The maximum and minimum variations in H₂O flux from cycle to cycle were repeatable. Table 4 lists the fluxes observed during this earlier period from 1969 to 1973 May reported by Schwartz *et al.* (1974). Of the five stars listed in Table 4, only one is within the range reported by Schwartz *et al.* (1974), U Her and U Ori have decreased by at least an order of magnitude in intensity, while W Hya has increased at least threefold.

In order to check the long-term variability of H₂O masers, observations of RX Boo and R Aql were made in 1977 December and observations of U Ori and W Hya were made in 1978 May and June, respectively, using the 42 m reflector of NRAO. No maser emission was detected from U Ori to a level of 1 Jy. A spectrum of R Aql from 1977 December is displayed in Figure 2. Figure 3 displays a spectrum of W Hya in 1978 June. The peak flux density of the 40 km s⁻¹ feature of half-width at half-maximum 0.25 km s⁻¹ is over 1900 Jy. In this spectrum, there are two other features, one at 38.8 km s⁻¹ of strength 190 Jy and half-width at half-maximum 0.45 km s⁻¹ and a weak broad feature 60 Jy centered at 40.5 km s⁻¹ of half-width at half-maximum 2.5 km s⁻¹. Gaussian line shapes were fitted in all three cases. U Ori was undetectable at 5 Jy peak to peak at the later epoch. R Aql was approximately at its light maximum at both observations, but

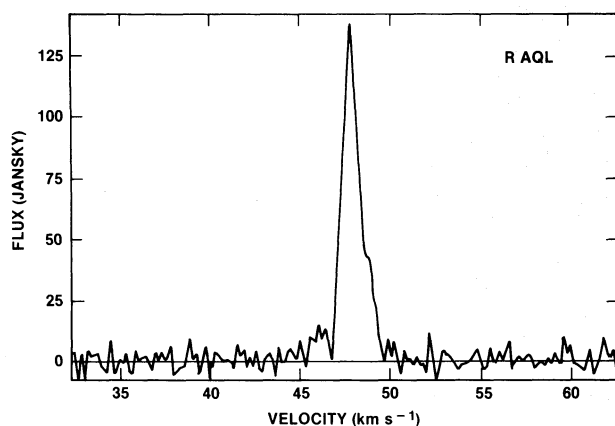


FIG. 2.—Spectrum of R Aql obtained in 1977 December. The velocity resolution is 0.21 km s⁻¹.

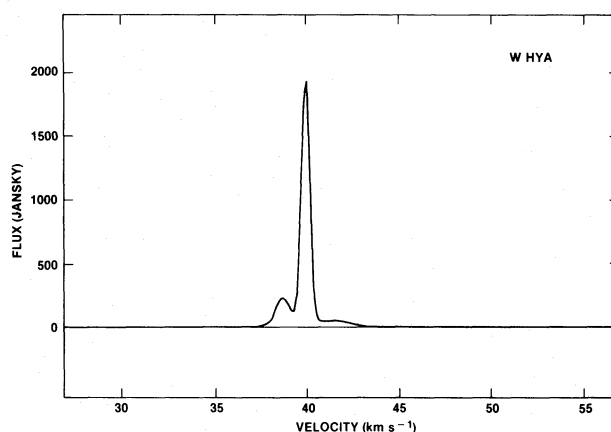


FIG. 3.—Spectrum of W Hya obtained in 1978 June. The velocity resolution is 0.21 km s⁻¹.

the maser power differed by a factor of 2. In the case of W Hya, the flux was a factor of 2 greater at a light phase of ~ 0.7 than it was at light maximum, although they were different cycles of this semi-regular star. This is greatly different from Schwartz *et al.* (1974), who display a correlation—not anticorrelation—between light curves and maser emission. More than our two data points are needed at current epochs, since our observations show that the maser emission is increasing. These changes in intensity appear to be long-term, on the order of years, and may correspond to large mass-loss events which alter the intensities of the OH and H₂O masers and should affect the IR flux considerably. The mass-loss process is not uniform, causing the observed changes in the H₂O maser emission. These changes in H₂O intensity should also imply similar substantial changes in the OH maser and infrared flux of these stars if the masers are pumped by IR photons as concluded by Schwartz *et al.* (1974). The 1612 OH maser emission from U Ori has decreased by a factor of 3 between 1975 January and 1978 January (Reid *et al.* 1979).

The weak broad feature in the 1978 June spectrum of W Hya is very similar to the weak quasi-thermal line observed in the $v = 0, J = 2-1$ SiO spectrum of W Hya (Buhl *et al.* 1975; Dickinson *et al.* 1978). Dickinson *et al.* (1978) find this SiO line centered at 40.0 km s⁻¹ with a strength of 0.36 K. They model this line as a thermal line centered on the stellar velocity. From the width of the line they estimate an expansion velocity of 8.6 km s⁻¹. We find no distance from the star, nor any temperature, where we can place a thermal shell that will fit both the SiO and the H₂O observations. If both lines originate in a shell of $\sim 10^4$ cm where the VLBI observations place the H₂O masers, both lines may be due to weakly pumped masers.

The 1977 December spectrum of RX Boo in Figure 4a represents a more complicated situation. We fitted five components to this spectrum using Gaussian profiles, although parabolas would be more appropriate for the broad features. They are shown in

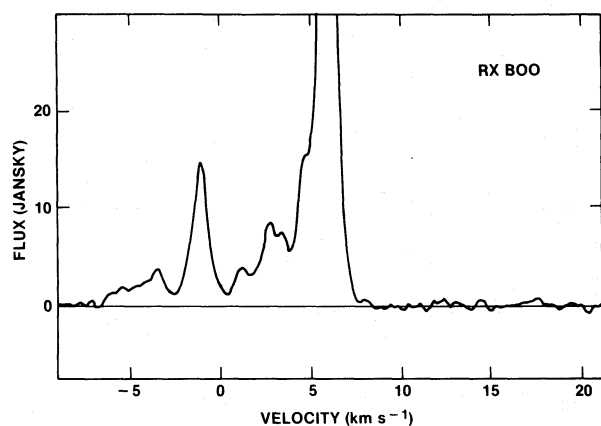


FIG. 4a

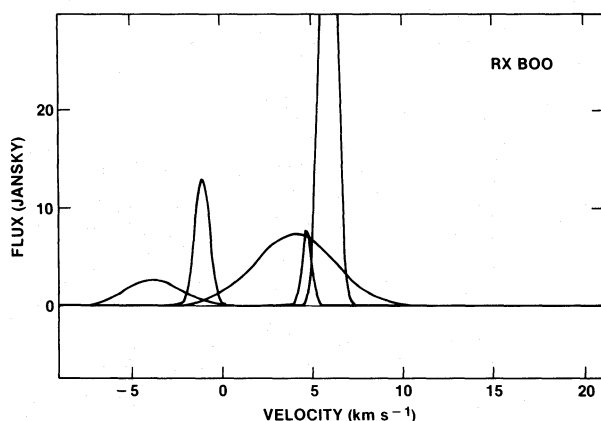


FIG. 4b

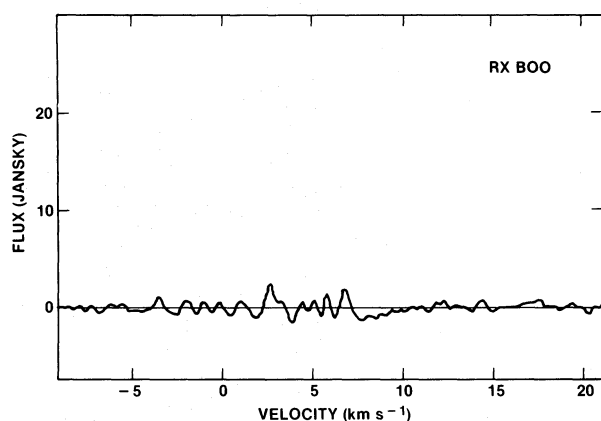


FIG. 4c

FIG. 4.—(a) Truncated spectrum of RX Boo obtained in 1977 December. The peak feature of 85 Jy is truncated to show the weak emission. (b) Five Gaussian components fitted to the spectrum. (c) Residuals after subtraction of the five components.

TABLE 5
COMPONENTS OF RX BOO IN 1977 DECEMBER

Component	Peak Flux Density (Jy)	Center Velocity (km s ⁻¹)	Half-width (km s ⁻¹)
1.....	75.4	5.7	0.46
2.....	6.9	3.1	2.0
3.....	13.9	-1.4	0.47
4.....	2.6	-4.0	1.9
5.....	10.3	4.5	0.3

Figure 4b, and the residual spectrum after their subtraction is shown in Figure 4c. The peak flux, center velocity, and Gaussian half-width at half-maximum of the components are presented in Table 5. Component 5 is most likely an artifact of our fitting Gaussian profiles. This is suggested by its location on the edge of component 1 and by the depression in the residuals near 8 km s⁻¹. There is a great resemblance in the relationship of components 1 to 2 and components 3 to 4. The velocity of component 2 agrees well with the optical absorption velocity of 3 km s⁻¹. Dickinson *et al.* (1978) reported the stellar velocity to be 0.3 ± 1.0 km s⁻¹ and the expansion velocity to be 10.3 ± 0.7 km s⁻¹. This is in good agreement with the midpoint between components 2 and 4. The reported expansion velocity is twice the velocity range of the H₂O components observed by us, suggesting that the H₂O masers do not occur at the largest radii of the SiO shell defined by the thermal radiation. As in the case of W Hya, the widths of the H₂O quasi-thermal components are narrower than the SiO, this time by a factor of 5.

IV. CONCLUSIONS

The H₂O maser emission for these variable stars has been found to be consistent with the present models of masers located in an expanding circumstellar shell. The stellar masers have larger apparent angular sizes and lower total luminosity, and they are distributed over a much smaller region than the H₂O masers in massive H II regions or even VY CMa. The amount of saturation for these masers is found to be much less than for the other objects. The maser emission is found to come from the front and back of a circumstellar shell in the case of W Hya. Long-term changes in the H₂O maser flux have been observed. Corresponding changes should be seen in the OH maser emission and iR flux from these objects if the maser emission is pumped by IR photons.

Radio astronomy research at the Haystack Observatory of the Northeast Radio Observatory is supported by the National Science Foundation. We thank the referee for his helpful comments and Janet Mattei of the American Association of Variable Star Observers for making light curves available.

REFERENCES

- Allen, C. W. 1973, *Astrophysical Quantities* (3d ed.; London: Athlone), p. 218.
- Buhl, D., Snyder, L. E., Lovas, F. J., and Johnson, D. R. 1975, *Ap. J. (Letters)*, **201**, L29.
- Clark, B. G. 1973, *Proc. IEEE*, **61**, 1242.
- de Jong, T. 1973, *Astr. Ap.*, **26**, 297.
- Dickinson, D. F. 1976, *Ap. J. Suppl.*, **30**, 259.
- Dickinson, D. F., Reid, M. J., Morris, M., and Redman, R. 1978, *Ap. J. (Letters)*, **220**, L113.
- Genzel, R., *et al.* 1978, *Astr. Ap.*, **66**, 13.
- Goldreich, P., and Scoville, N. 1976, *Ap. J.*, **205**, 144.
- Johnston, K. J., Knowles, S. H., Moran, J. M., Burke, B. F., Lo, K. Y., Papadopoulos, G. D., Read, R. B., and Hardebeck, E. G. 1977, *A.J.*, **82**, 403.
- Labeyrie, A., Koechlin, L., Bonneau, D., Blazit, A., and Foy, R. 1977, *Ap. J. (Letters)*, **218**, L75.
- Lang, R., and Bender, P. L. 1973, *Ap. J.*, **180**, 647.
- Lepine, J. R. D., Paes de Barros, M. H., and Gammon, R. M. 1976, *Astr. Ap.*, **48**, 269.
- Mader, G. L., and Johnston, K. J. 1973, private communication.
- Moran, J. M. 1973, *Proc. IEEE*, **61**, 1236.
- Moran, J. M., *et al.* 1973, *Ap. J.*, **185**, 535.
- Olnon, F. M. 1977, Ph.D. thesis, Leiden University.
- Reid, M. J., Moran, J. M., Ball, J., Johnston, K. J., and Spencer, J. H. 1979, *Ap. J.*, submitted.
- Rosen, B. F., Moran, J. M., Reid, M. J., Walker, R. C., Burke, B. F., Johnston, K. J., and Spencer, J. H. 1978, *Ap. J.*, **222**, 132.
- Schwartz, P. R., Harvey, P. M., and Barrett, A. H. 1974, *Ap. J.*, **187**, 491.
- Walker, R. C., *et al.* 1978, *Ap. J.*, **226**, 95.

K. J. JOHNSTON and J. H. SPENCER: Code 7134, Naval Research Laboratory, Washington, D.C. 20375

J. M. MORAN: Smithsonian Astrophysical Observatory, 60 Garden Street, Cambridge, MA 02138

M. J. REID: National Radio Astronomy Observatory, Edgemont Road, Charlottesville, VA 22901

R. C. WALKER: Astronomy Department, California Institute of Technology, Pasadena, CA 91125